Accepted in J. Phys. D: Appl. Phys, 38 1978-1983 (2005), doi:10.1088/0022-3727/38/12/018.

Simultaneous determination of mass and thermal accommodation coefficients from temporal evolution of an evaporating water microdroplet

M Zientara, D Jakubczyk, G Derkachov, K Kolwas and M Kolwas

Institute of Physics of the Polish Academy of Sciences, al.Lotników 32/46, 02-668 Warsaw, Poland

E-mail: jakub@ifpan.edu.pl

Abstract. Scattering of coherent light by an evaporating droplet of pure water several micrometres in size was investigated. The droplet was levitated in an electrodynamic trap placed in a small climatic chamber. The evolution of droplet radius and the evolution dynamics was investigated by means of analysing the scattering patterns with the aid of Mie theory. A numerical model of droplet evolution, incorporating the kinetic effects near the droplet surface was constructed. Application of this model to the experimental data allowed us to determine the mass and thermal accommodation coefficients to be $\alpha_C = 0.12 \pm 0.02$ and $\alpha_T = 0.65 \pm 0.09$ respectively. This model enabled us to determine with high precision the temperature evolution of the droplet and the relative humidity in the droplet vicinity.

PACS numbers: 68.03.Cd, 68.03.Fg

Submitted to: *J. Phys. D: Appl. Phys.*

1. Introduction

The processes of evaporation and condensation are at the very heart of many fields of science. Cloud and aerosol microphysics together with construction of climate models [1], electrospraying and combustion are just some areas of relevance. Such processes are typically modelled with diffusion type mass and heat transport equations. In many cases the evolution of droplets of size comparable to the mean free path of surrounding gas molecules must be considered. This in turn requires accounting for the kinetic effects. It is then necessary to supplement the diffusion coefficient with a so called evaporation (condensation) or mass accommodation coefficient α_C. Likewise the thermal conductivity coefficient is supplemented with a thermal accommodation coefficient α_T. These coefficients describe the transport properties of the liquid-gas interface. The mass accommodation coefficient can be perceived as the probability

that a molecule (e.g. water) impinging on the interface from the gaseous phase side enters into the bulk liquid phase and does not rebound. Analogically, the thermal accommodation coefficient determines the probability that a molecule impinging on the interface attains thermal equilibrium with the medium on the opposite side. The coefficients of transport in opposite directions are considered to be equal [2]. Both coefficients are phenomenological and should describe only the properties of the very interface. All other processes influencing mass and heat transport, such as chemistry of the interface or the electrostatic interactions should be accounted for separately [3]. It is agreed, however, that α_C and α_T might possibly exhibit some temperature dependence [2].

Many attempts to determine the values of α_C and α_T for water have been made over nearly a century, but the results obtained by different authors were rather ambiguous. Values ranging from 0.01 to 1 for α_C and from 0.5 to 1 for α_T have been reported [2, 4, 5, 6, 7, 8, 9, 10, 11, 12]. Some authors differentiated between a new and an aged water surface, which indicates difficulties in extracting pure coefficients and accounting for various processes involved. Determining α_C and α_T simultaneously also seems to have presented some difficulty [11].

In this paper we present a method for determining α_C and α_T simultaneously as well as the first results of applying it to pure water. The method is based on the analysis of evaporation of a microdroplet of water in a humid environment. The size of the droplet as the function of time was determined by analysing the Mie scattering patterns with the aid of a precise, Mie theory based, procedure.

2. Experiment

The experimental setup is presented in figure 1 and consists of an electrodynamic quadrupole trap [13] kept in a small climatic chamber. Detailed description of this apparatus can be found in [14] and of further modifications in [15, 16].

Temperature in the upper and in the lower part of the chamber was measured (T-type thermocouple, TT-T-40-SLE, Omega) and controlled separately. Such setup enabled us to eliminate vertical temperature gradients. Horizontal gradients were found to be negligible. There were also two relative humidity sensors (HIH3610-2, Honeywell): above and below the trap.

Before each experiment, the chamber was flushed with dry gaseous nitrogen, obtained from above liquid nitrogen, in order to remove liquid water that accumulates in the chamber during experiments due to condensation and stray injection. Next, a filtered humid air (obtained by bubbling through distilled water) was passed through the chamber from the bottom to the top port. When the required humidity and a satisfactory humidity gradient were reached, the flow was stopped to enable uninfluenced trapping. Between the instants of trapping the chamber was flushed with humid air to maintain required humidity conditions.

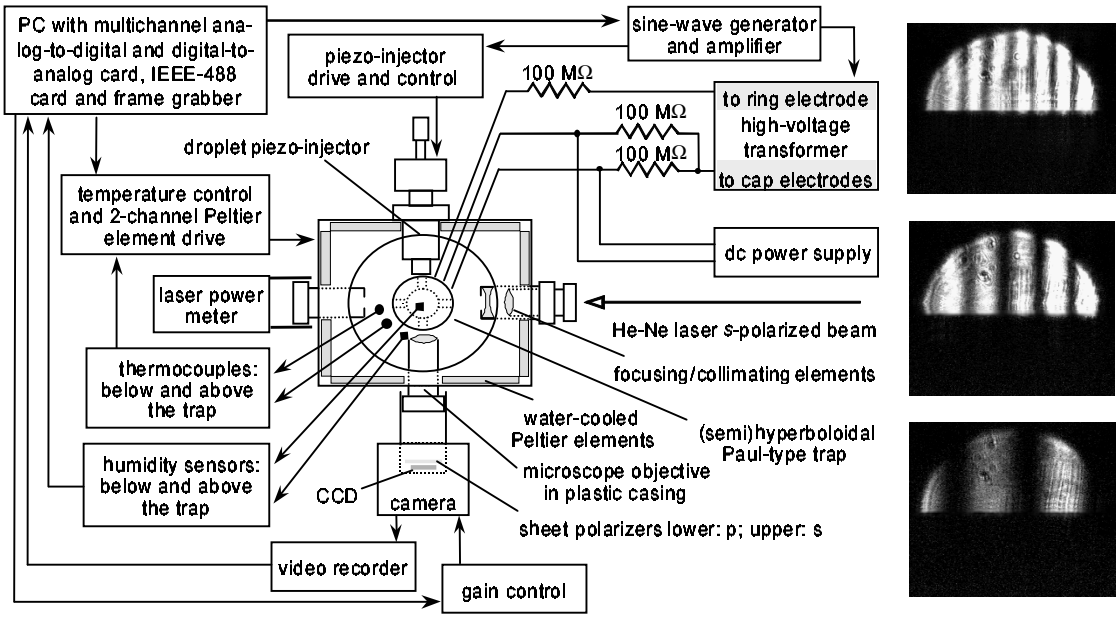

Figure 1. Left: experimental setup. Right: three example scatterograms recorded in (starting from the topmost) 2nd, 7th and 11th second of an experiment.

2.1. Thermodynamic conditions and sample preparation

The thermodynamic conditions of experiments presented in this paper were: atmospheric pressure 1006 hPa (public meteorological data), climatic chamber temperature - we worked at 2 slightly different temperatures - 286.3 ± 0.5 K and 286.9 ± 0.5 K, vertical temperature gradient between the sensors below 0.3 K and average sensor measured relative humidity of 88, 89 and 90%.

Ultra pure water was produced locally (Milli-Q Plus, Millipore). A sterile plastic syringe, additionally washed with ultra pure water, was used for transferring it into the droplet injector within 10 minutes, and the experiment was conducted within 1 hour after (ultra) purification.

The initial parameters of the ultra pure water we used, guaranteed by the equipment manufacturer, were: resistivity $\sim$ 18 MΩcm, total dissolved solids $<$ 20 ppb, total organic carbon (TOC) $\leq$ 10 ppb, no suspended particles larger than 0.22 μm, microorganisms $\leq$ 1 cfu/ml (colony forming unit per ml), silicates $<$ 0.1 ppb and heavy metals $\leq$ 1 ppb. Since the influence of even small amounts of surface active agents upon the experimental results might be disproportionately large, we tried to estimate it in our case. On assuming that all TOC comes from surfactants and that it is all concentrated in $\sim$1 nm layer on the surface of the droplet, we still arrive at $\sim$30 ppm of surfactant in this layer for a droplet of 8 μm radius (average initial radius in our experiment - see section 4). If we assume that the mass of the surfactant molecule is equal to (only) 10 masses of the water molecule, than there are $\sim 3 \times 10^5$ water molecules per one surfactant molecule. During the evaporation droplet radius diminishes, on

average, by a factor of 5, so concentration of surfactant grows by a factor of 25 (we assume that the thickness of the surface layer does not change). This yields $\sim 10^4$ water molecules per surfactant molecule for freshly purified water. Thus, the influence of surface active agents upon evaporation rate at this stage is not expected to be of importance. We were not able to determine how the water during the transfer and the experiment was picking up contaminants of non-ionic kind. However we carefully measured the changes of resistivity of ultra pure water loaded into the injector (made of Pyrex glass and Plexiglass) and were able to estimate how this water sample was picking up contaminants of ionic kind. We found out that during the first hour the concentration of such impurities grew by a factor of 3, which together with ~ 125 times increase of (volume) concentration during droplet evaporation, still by itself has undetectable influence upon the evolution of the droplet (see the rightmost hand term of equation 2). If we assume, by similarity, that the concentration of surfactants grows by a factor of 3 over the same time interval, we obtain $\sim 3 \times 10^3$ water molecules per surfactant molecule (0.003 surfactant mass concentration) at the end of the evolution of the droplet, which still seems reasonable. We observed that in about 10 hour time the total concentration of all dissolved substances was becoming large enough to stop the evaporation of the droplet. At the current stage we can not point to a specific agent responsible for this. According to our resistivity measurements there would then be ~ 45 ppb of impurities of ionic kind. The influence of the city atmosphere, containing such gases as CO_2 or SO_2, upon the levitating droplet should also be kept in mind.

2.2. Determination of evolution of droplet radius

The upper and lower halves of the scatterogram recorded during the experiment present the scattered light intensity I for p (vertical) and ps (depolarisation) polarisations respectively, as a function of azimuth angle θ in the observation plane and elevation angle ϕ (see e.g. [17]). The observation in the ps configuration enabled us to detect solid impurities acquired by the droplet and reject the affected data. Three example scatterograms are presented in figure 1. The scatterogram was averaged vertically yielding the $I(\theta)$ function which was further smoothed with an FFT filter. We then fitted the experimental $I(\theta)$ with the theoretical $I_T(\theta)$ dependence generated with Mie formulae, for all video frames, and found the evolution of the droplet radius $a(t)$ (see: figure 3). The fitting was performed with a gradientless library method, where the smallest value of the functional

$$P(a,\beta) = \int_{\theta_1}^{\theta_2} \left[\frac{I(\theta)}{\max_{\theta_1<\theta<\theta_2} I(\theta)} - \frac{I_T(a,\theta-\beta)}{\max_{\theta_1<\theta<\theta_2} I_T(\theta)} \right] d\theta \qquad (1)$$

is sought. θ_1 and θ_2 determine the effective field of view and β is the angle of displacement accounting for side movements of the droplet in the trap. Application of this method to our experimental data allowed us to find $a(t)$ with ± 25 nm (i.e. $\leq 1\%$) precision.

3. Model

3.1. Evaporation of a droplet

Many authors have discussed droplet evaporation, by also taking kinetic effects into account (see e.g.: [2, 10, 18, 19]). The model we utilised was a slightly rephrased version of that presented in [2] with kinetic and surface tension effects emphasised. We also incorporated the effect of droplet charge and of soluble contaminants (compare e.g.: [20, 21]).

The steady state evaporation of a charged droplet is governed by mass and heat transport equations:

$$\begin{aligned}\dot{a} &= \frac{M D_k(a,T_a)}{Ra\rho_L} \times \\ &\times \left\{ S\frac{p_s(T_R)}{T_R} - \frac{p_s(T_a)}{T_a} \exp\left[\frac{M}{RT_a\rho_L}\left(\frac{2\gamma}{a} - \frac{Q^2}{32\pi^2\varepsilon_0 a^4} \right) - n_s \frac{a_0^3}{a^3} \right] \right\}, \quad (2)\end{aligned}$$

$$\dot{T}_a = \frac{3}{a^2 c_w}\left[qa\dot{a} - \frac{\lambda_K(a,T_a)}{\rho_L}(T_a - T_R) \right], \quad (3)$$

where a, a_0, T_a and Q are the droplet radius, initial radius, temperature and charge respectively; T_R and S are the temperature and relative humidity far from the droplet (the reservoir volume is more than 10^{64} times larger than that of the droplet), p_s is the saturated vapour pressure at a given temperature, ρ_L and γ are the density and surface tension of liquid water respectively, ε_0 is the permittivity of vacuum, M is the molecular mass of water, n_s is the concentration of soluble contaminants and R is the universal gas constant. The influence of soluble contaminants was considered within the limit of very low concentrations. The effective diffusion coefficient and the effective thermal conductivity of moist air account for gas kinetic effects which take place up to a distance from the droplet surface comparable to the mean free path of molecules of gases present in the air:

$$D_k = \frac{D}{a/(a+\Delta_C) + D\sqrt{2\pi M/(RT_a)}/(a\alpha)}\ , \quad (4)$$

$$\lambda_K = \frac{\lambda}{a/(a+\Delta_T) + \lambda\sqrt{2\pi M_A/(RT_a)}/(a\alpha_T\rho_A c_P)}\ , \quad (5)$$

where $\Delta_C \approx 1.3\lambda_a$, λ_a is the mean free path of air molecules, Δ_T is the 'thermal jump' distance, D is the diffusion constant for water vapour in air, c_w and q are specific heat capacity and latent heat of evaporation of water respectively, λ, ρ_A, c_P and M_A are thermal conductivity, density, specific heat capacity under constant pressure and molecular mass of moist air respectively.

Equations 2–3 must be supplemented with the Rayleigh condition [22]

$$\frac{E_Q}{2E_\gamma} = \frac{Q^2}{64\pi^2\varepsilon_0\gamma a^3} < 1 \quad (6)$$

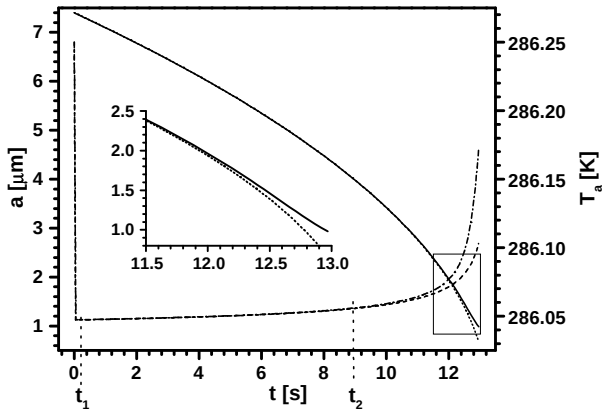

Figure 2. Numerical simulation of the evolution of water droplet radius (solid and dotted lines) and of droplet temperature (dash and dash-dot lines). Dotted and dash-dotted lines, only surface tension taken into account in the exponential term of equation 2; solid and dashed lines, the effects of charge and contaminants taken into account as well. The departure region, for $a(t)$, is shown enlarged in the inset. $T_a(t)$ can be linearly approximated between t_1 and t_2. Model parameters: $p_{atm} = 1006$ hPa, $T_R = 286.25$ K, $a_0 = 7.4$ μm, $Q = 4 \times 10^5$ elementary charge units, $n_s = 100$ ppb, $S = 0.978$, $\alpha_C = 0.12$ and $\alpha_T = 0.62$.

where E_Q is the Coulomb energy of a charged droplet and E_γ is the energy associated with the surface tension.

The evolution of the droplet is driven by the gradients of temperature and water vapour density near the droplet surface. Since the droplet injector nozzle remains at the temperature of the chamber, then the initial temperature of the droplet is the same: $T_a(0) = T_R$. It is clear that the initial vapour density is uniform across the chamber. A droplet of pure water is not in equilibrium with its surroundings for such conditions for $S \leq 1$. The fastest molecules leave the liquid phase for the vapour and thus the evaporation starts at the cost of the droplet internal energy. However in a fraction of a second the evaporation reaches its nearly steady state. Neutral droplets evaporate completely. Charged droplets evaporate until Coulomb explosion occurs. For the droplets of a solution a stabilisation of the size is possible since the increase of concentration lowers the (equilibrium) vapour pressure over the surface of the solution.

The model presented above has been tested numerically for water (see figure 2). The values of constants pertaining to water properties were taken from [2, 23, 24, 25, 26, 27] and the values of $\Delta_C = 10.4 \times 10^{-8}$ m and $\Delta_T = 2.16 \times 10^{-7}$ m were taken from [2]. The influence of temperature dependence of λ, ρ_L, D and γ as well as of those for c_w, q and λ_a upon the solution of the set 2-3 for 233 K$< T_R <$ 313 K was found to be below 0.5% and was considered negligible [23, 24, 25, 28]. The departure of droplet surface temperature from the temperature of the reservoir $T_a - T_R$ was always well below 1 K.

3.2. Determination of α_C and α_T

It can be easily noted (see figure 2), that for steady state evaporation, for the range of time $t_1 < t < t_2$, $T_a(t)$ can be treated as a linear function of time. For this interval it can be assumed that all of the heat flowing into the droplet is used up for evaporation. Equation 3 can then be simplified considerably and presented in the following form:

$$Bt + C = T_R + a\dot{a}\frac{q\rho_L}{\lambda_K} \ , \tag{7}$$

where B and C are constants. From the experiment we obtained $a(t)$ and were able to calculate $a\dot{a}(t)$. The quantities p_{atm} and T_R were also measured. For any 3 points in time between t_1 and t_2 it is possible to obtain a solvable equation set and find B, C and α_T (by finding λ_K). By taking all triples with reasonable spacing between the points, that yielded $A > 0$, $B > 0$ and $0 < \alpha_T < 1$, we obtained a statistical distribution of α_T. We fitted it with a normal distribution and thus obtained a most probable value of α_T and the distribution half-width which reflects statistical accuracy. By inserting α_T into equation 7 we were able to find $T_a(t)$.

For $t_1 < t < t_2$ the influence of the droplet charge and dissolved contaminants (at the concentration possible in our case) upon the solution of equations set 2-3 is negligible. On insertion of $T_a(t)$ and $a\dot{a}$ into equation 2 it is again possible to obtain for any 2 points between t_1 and t_2 a solvable equation set. By applying the procedure described above we found α_C and S and estimated their accuracy. We again used only the solutions satisfying the conditions $0 \leq S \leq 1$ and $0 < \alpha_T \leq 1$.

In order to verify our approach we inserted α_C, α_T and S back into the model for direct calculation of $a(t)$ and $T_a(t)$. The results presented in figure 3 prove the self-consistency of our approach.

4. Results

We selected five data sets collected under thermodynamic conditions given in section 2.1. The regions of droplet radii for which we applied our method were: 10740 nm $\rightarrow$ 3740 nm, 9700 nm $\rightarrow$ 1790 nm, 7360 nm $\rightarrow$ 1800 nm, 7340 nm $\rightarrow$ 1500 nm and 7000 nm $\rightarrow$ 1000 nm. We obtained the value of $\alpha_C = 0.12 \pm 0.02$ fivefold and an average value of $\alpha_T = 0.65 \pm 0.09$. The relative humidity S found simultaneously with α_C also varied from set to set in the range of $(0.974 \div 0.983) \pm 0.009$. The evolution of the droplet is extremely sensitive ($< 10^{-3}$) to S which makes checking the obtained values with a probe very difficult (accuracy of instruments does not exceed 10^{-2}) [29]. In figure 3 we also present the evolution of droplet temperature. Though experimentally obtained $a(t)$ seems quite smooth, there still is some noise which manifests plainly in $\dot{a}(t)$, even after further smoothing (FFT filtering), and so is inherited by $T_a(t)$. However, it is worth noting that the fluctuations are at the level of several mK, which corresponds to $\sim 10^{-4}$ relative error. Further improvement requires experimental data of still better quality.

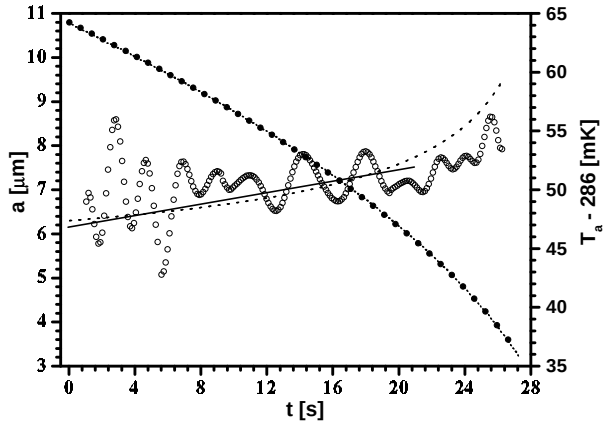

Figure 3. Experimentally determined evolution of droplet radius (solid circles) and temperature (hollow circles). Linear approximation of $T_a(t)$ is shown in solid line. Numerical calculations (dotted and dashed lines) are for parameters determined from the experiment. Specific experimental conditions: $T_R = 286.3$ K, the average relative humidity measured with sensors was 90% and the relative humidity determined from the evolution dynamics $S = 0.9805$.

4.1. Discussion

The presented values of mass and thermal accommodation coefficients are not direct experimental numbers but depend on the underlying model. There are a few issues that should be discussed.

(i) The process of evaporation can not be considered to be a steady state one all the time, and propagation of mass and heat waves should be taken into consideration. However, evaporation is non stationary for several milliseconds [2] and this phase has negligible impact on further stationary process. This briefly lasting non stationary phase was not accessible at all in our experiment.

(ii) In part of the model considerations we made another approximation of a similar kind. As we mentioned in section 3.2, we neglected the influence of the heat capacity of the droplet. We checked numerically that for $t_1 < t < t_2$ when the temperature of the droplet is nearly constant (see figure 2) such simplification is justified.

(iii) The matching of gas kinetic and diffusional regime is an essential part of the model. The similarity of mathematical formulas describing both regimes is utilised and the parameters Δ_C and Δ_T are introduced to describe the points at which the exact matching takes place. However it is obvious that physically they are rather regions than points. And indeed, we checked numerically that changing just Δ_T by a factor of up to 4 or Δ_C by a factor of up to 40 has a negligible effect upon the evolution of $a(t)$ or $T(t)$.

(iv) There are many constants (taken from the literature) and parameters of the model which are known with finite accuracy. This certainly might influence the accuracy of finding α_C and α_T. However, we found that the accuracy of determining droplet radius has, mainly through the action of derivative, a much greater impact upon the accuracy of α_C and α_T than any other constant or parameter. The accuracy with which the

temperature and pressure of droplet surroundings are measured has a negligible impact upon the accuracy of α_C and α_T but weights upon S. Apart from that, the direct fitting of the model to the experimental data seems to suggest that the accuracy of temperature measurements is better (± 0.2 K) than guaranteed by the thermocouple manufacturer.

5. Conclusion

We have presented a method of simultaneous determination of α_C and α_T. It is based on the analysis of the dynamics of the evolution of radius of the evaporating droplet. The method was applied to a few sets of experimental data and yielded values consistent with other authors' results [6, 7, 8, 11, 12]. We were also able to find the evolution of the droplet temperature and the relative humidity of the droplet surroundings with a very high precision.

We intend to extend our investigations to lower pressures and cover a wider range of temperatures. In this way we shall be able to study the temperature dependence of α_C and α_T also for longer mean free paths of air constituting molecules when the kinetic effects prevail. We intend to use nitrogen and CO_2 atmospheres as well in order to investigate the role of contaminants in the water arising from the standard atmosphere.

Acknowledgments

This work was supported by Polish State Committee for Scientific Research grant 2 P03B 102 22.

References

[1] Garratt J R, Rotstayn L D and Krummel P B 2002 The atmospheric boundary layer in the CSIRO global climate model: simulations versus observations *Climate Dynamics* **19** 397-415

[2] Pruppacher H R and Klett J D 1997 *Microphysics of Clouds and Precipitation* (Dordrecht: Kluwer)

[3] Shi Q, Davidovits P, Jayne J T, Worsnop D R and Kolb C E 1999 Uptake of gas-phase ammonia. 1. Uptake by aqueous surfaces as a function of Ph *J Phys Chem A* **103** 8812-23

[4] Winkler P M, Vrtala A, Wagner P E, Kulmala M, Lehtinen K E J and Vesala T 2004 Mass and thermal accommodation during gas-liquid condensation of water *Phys Rev Lett* **93** 75701-1-4

[5] Vieceli J, Roeselová M, Tobias D J 2004 Accommodation coefficients for water vapor at the air/water interface *Chem Phys Lett* **393** 249-55

[6] Hagen D E, Schmitt J, Trublood M, Carstens J, White D R and Alofs D J 1989 Condensation coefficient measurement for water in the UMR cloud simulation chamber *J Atmos Sci* **46** 803-16

[7] Zagaynow V A, Nuzhny V M, Cheeusova T A and Lushnikov A A 2000 Evaporation of water droplet and condensation coefficient: theory and experiment *J Aerosol Sci* **31** suppl 795-6

[8] Sageev G, Flagan R C, Seinfeld J H and Arnold S 1986 Condensation of water on aqueous droplets in the transition regime *J Colloid Inreface Sci* **113** 421-9

[9] Gollub J P, Chabay I and Flygare W H 1974 Laser heterodyne study of water droplet growth *J. Chem. Phys.* **61**, 2139-44

[10] Zou Y S and Fukuta N 1999 The Effect of Diffusion Kinetics on the Supersaturation in Clouds *Atm Research* **52** 115-41

[11] Shaw R A and Lamb D 1999 Experimental determination of the thermal accommodation and condensation coefficients of water *J Chem Phys* **111** 10659-63
[12] Li Y Q, Davidovits P, Shi Q, Jayne J T, Kolb C E and Worsnop D R 2001 Mass and thermal accommodation coefficients of H_2O (g) on liquid water as function of temperature *J Phys Chem A* **105** 10627-34
[13] Paul W 1990 Electromagnetic traps for charged and neutral particles *Rev Mod Phys* **62** 531-40
[14] Jakubczyk D, Zientara M, Bazhan W, Kolwas M and Kolwas K 2001 A device for light scatterometry on single levitated droplets *Opto-Electron Rev* **9** 423-30
[15] Jakubczyk D, Derkachov G, Bazhan W, Łusakowska E, Kolwas K and Kolwas M 2004 Study of microscopic properties of water fullerene suspensions by means of resonant light scattering analysis *J. Phys. D* **37** 2918-24
[16] Jakubczyk D, Derkachov G, Zientara M, Kolwas M and Kolwas K 2004 Local-field resonance in light scattering by a single water droplet with spherical dielectric inclusions *J. Opt. Soc. Am. A* **21** (in print)
[17] Born M and Wolf E 1970 *Principles of Optics* (Oxford: Pergamon)
[18] Fuchs N A 1959 *Evaporation and Droplet Growth in Gaseous Media* (London: Pergamon)
[19] Kozyrev A V and Sitnikov A G 2001 Evaporation of a spherical drop in a middle pressure gas *Uspekhi Fizicheskikh Nauk* **171**, 765-74
[20] Friedlander S K 2000 *Smoke, Dust and Haze Fundamentals of Aerosol Dynamics* (New York, Oxford: Oxford University Press)
[21] Cadle R D 1966 *Particles in the Atmosphere and Space* (New York: Reinhold Publishing Corporation)
[22] Durft D, Lebius H, Huber B A, Guet C and Leisner T 2002 Shape oscillations and stability of charged microdroplets *Phys Rev Lett* **89** 84503-1-4
[23] 1999 Revised Release on the IAPS Formulation 1985 for the Thermal Condactivity of Ordinary Water Substance, The International Association for the Properties of Water and Steam (London)
[24] 1992 Revised Supplemantary Release on Saturation Properties of Ordinary Water Substance, The International Association for the Properties of Water and Steam (St. Petersburg)
[25] 1994 IAPWS Revised on Surface Tension of Ordinary Water Substance, The International Association for the Properties of Water and Steam
[26] Harvey A H, Gallagher J S and Levelt Sangers J M H 1998 Revised formulation for the refractive index of water and steam as function of wavelenght, temperature and density *J Phys Chem Ref Data* **27** 761-75
[27] Rasmussen K 1997 Calculation Methods for the Physical Properties of Air Used in the Calibration Microphones. A Proposal for Unified Calibration Procedure to Be Used Among European Metrology Laboratories *www.dat.dtu.dk/docs/PL11b-RAP.PDF*
[28] Hall W D and Pruppacher H R 1976 The survival of ice particles falling from cirrus clouds in subsaturated air *J. Atmos.Sci.* **33** 1995-2006
[29] Wiederhold P R 1997 *Water Vapor Measurement, Methods and Instrumentation* (New York: Marcel Dekker)